JURNAL REKAYASA PROSES
VOLUME 19, NUMBER 1, 2025, 58–65

RESEARCH ARTICLE

# Synthesis of hydroxyapatite from hard clams shell (Meretrix spp.) using hydrothermal method as a dental implant coating biomaterials

Zefania Riri[1], Patrinela Hilda[1], Lalak Tarbiyatun Nasyin Maleiva[1,*], Intan Syahbanu[2], Syahrul Khairi[1], Kiki Aristi[1]

[1]Department of Chemical Engineering, Faculty of Engineering, Tanjungpura University, Jalan Jenderal Ahmad Yani, Bansir Laut, Pontianak Tenggara, Pontianak 78124, Indonesia
[2]Department of Chemistry, Faculty of Mathematics and Natural Sciences, Tanjungpura University, Jalan Jenderal Ahmad Yani, Bansir Laut, Pontianak Tenggara, Pontianak 78124, Indonesia

Received 09 December 2024; revised 22 January 2025; accepted 07 March 2025


OBJECTIVES Hydroxyapatite (HAp) is a biomaterial widely used as a coating for dental implants due to its biocompatibility and structural similarity to natural bone. METHODS This study explores the synthesis of HAp using ale-ale shell waste as a natural calcium source through the hydrothermal method. The synthesis was conducted by varying the $CaO/(NH_4)2HPO_4$ concentration ratios (0.67; 1.67; 2.67) and pH levels (11, 12, 13) to optimize crystal formation. FTIR analysis confirmed the presence of key functional groups characteristic of HAp, while XRD analysis validated the formation of a crystalline structure matching standard hydroxyapatite. RESULTS The results demonstrate that the hydrothermal method effectively converts ale-ale shell waste into HAp with high crystallinity, suggesting its potential as a sustainable biomaterial for biomedical applications. CONCLUSIONS The optimal synthesis conditions were achieved at a $CaO/(NH_4)2HPO_4$ concentration ratio of 2.67 and pH 13, producing HAp with favorable properties for dental implant coatings.

KEYWORDS ale-ale; dental implant; hydroxyapatite; hydrothermal

## 1. INTRODUCTION

Dental and oral health is still a problem in society that needs attention. According to the latest data from the 2023 Indonesia Health Survey (SKI), the prevalence of oral and dental health problems in Indonesia is 56.9%, reflecting a 0.7% decrease from 57.6% in 2018. Additionally, the prevalence of dental caries has also declined from 88.8% in 2018 to 82.8% in 2023. Despite this decrease, the figures still indicate that more than half of the Indonesian population experiences oral and dental health issues. The most common attempt to improve the function of these teeth is to use dental implants. An implant material that is widely used in the field of orthopedics and dentistry is a type of titanium alloy. Titanium (Ti) has low density, high strength, and bioinert properties. However, titanium has its shortcomings, namely, that particles and ions of Titan, as well as the components of the alloy, can accumulate in the surrounding tissues due to corrosion and weariness, resulting in inflammatory reactions (Souza et al. 2019). Given the level of danger caused by the use of titanium alloy-based implants, many dental implants have been modified with coatings using biomaterials. Biomaterials that can be used as coatings on dental implants are hydroxyapatites. Hydroxyapatite (HAp), $Ca_{10}(PO_4)_6(OH)_2$, is a major mineral found in bones and teeth. One of the natural ingredients used in the synthesis of hydroxyapatite is the shell because it has a high calcium carbonate composition, i.e. about 89% that can be used as a source of calcium to synthesize compounds containing calcium metals such as hydroxyapatite (Affandi et al. 2015).

The ale-ale shell (Meretrix spp.) is a hard clams shell as a freshwater mollusk endemic in Ketapang District, West Kalimantan of Indonesia. Ale-ale shells are known to have a high calcium content of 87.139 % (Fadhilah et al. 2015). This significant calcium concentration makes Meretrix spp. shells a promising raw material for hydroxyapatite synthesis, as calcium is a key component in hydroxyapatite formation. Among several methods of hydroxyapatite synthesis, the hydrothermal method is the most advantageous because it can produce hydroxyapatite with high levels of crystallinity and purity, as well as a homogeneous material size distribution. Besides, the hydrothermal method is relatively simple without the use of complicated and expensive equipment (Sianipar et al. 2016). However, previous studies on hydroxyapatite synthesis using the hydrothermal method have primarily focused on variations in temperature, pressure, and reaction

*Correspondence: lalaktnm@teknik.untan.ac.id

time, without thoroughly exploring the effects of pH and the $CaO/(NH_4)_2HPO_4$ concentration ratio, particularly when using calcium derived from ale-ale shells. This study aims to fill this gap by investigating these specific parameters, thereby contributing to the originality of the research and enhancing the potential application of ale-ale shell-derived hydroxyapatite for biomedical purposes, such as dental implant coatings that comply with ICDD standard 01-072-1243 (International Centre for Diffraction Data). Through this standard, a comparison of the characteristics of synthetic hydroxyapatite that can be used as a dental implant coating can be made.

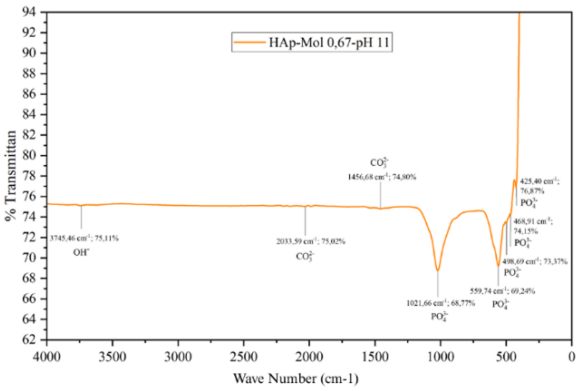


FIGURE 1. FTIR spectrum of HAp with $CaO/(NH_4)2HPO_4$ concentration ratio of 0.67 and pH 11.

## 2. MATERIALS AND METHODS

### 2.1 Materials

This research was conducted using an experimental quantitative method over four months at the Integrated Chemical Laboratory of Tanjungpura University, Pontianak. The primary material used was ale-ale shells obtained from Ketapang District. Other materials included water, aluminum foil, filing paper, ammonium phosphate ($(NH_4)_2HPO_4$), ammonium hydroxide ($NH_4OH$), and wrapping plastic.

The instruments used in this study included a mortar and pestle, 200-mesh sieve, stirring rod, Buchner funnel, Erlenmeyer flask, furnace, beaker glass, measuring cylinder, analytical balance, oven, pH meter, pipette filler, drop pipette, volumetric pipette, vacuum pump, hydrothermal reactor, spatula, and characterization instruments such as X-ray fluorescence (XRF), Fourier-transform infrared spectroscopy (FTIR), and X-ray diffraction (XRD).

### 2.2 Methods

#### 2.2.1 Hard clams shell preparation

The preparation of the hydroxyapatite precursor followed the method described by Fadhilah et al. (2015). Ale-ale shells were first cleaned, boiled, dried, and ground to a particle size of 200 mesh. The obtained powder was then calcined at 900 °C for 4 hours in an open-air atmosphere furnace to remove volatile compounds and enhance calcium oxide (CaO) purity. Gradual heating was applied to prevent structural degradation, followed by slow cooling inside the furnace to maintain phase stability. The resulting material was analyzed using X-ray fluorescence (XRF) to determine its elemental composition, ensuring optimal CaO formation for hydroxyapatite synthesis.

#### 2.2.2 Hydroxyapatite synthesis

The hydroxyapatite synthesis followed the procedure outlined by Affandi et al. (2015), in which a mixture of calcium hydroxide ($Ca(OH)_2$) solution and diammonium hydrogen phosphate ($(NH_4)_2HPO_4$) solution was prepared with $CaO/(NH_4)_2HPO_4$ concentration ratios of 0.67; 1.67; and 2.67. These ratios corresponded to molar ratios of 2:3, 5:3, and 8:3, respectively, resulting in Ca/P molar ratios of 0.67; 1.67; and 2.67. The molar ratio was determined based on the number of moles of each precursor used in the reaction. Calcium was sourced from $Ca(OH)_2$ solution, with molar amounts of 0.075; 0.14; and 0.18 mol, corresponding to 5.544 g, 10.381 g, and 13.457 g of $Ca(OH)_2$ powder, respectively. Meanwhile, phosphate was derived from $(NH_4)_2HPO_4$ solution, with molar amounts of 0.1125; 0.075; and 0.05625 mol, corresponding to 19.602 g, 14.652 g, and 11.88 g of $(NH_4)_2HPO_4$ powder, respectively. The pH of the mixture was then adjusted to 11, 12, and 13 by adding $NH_4OH$ to optimize hydroxyapatite formation. The prepared solution was transferred into a hydrothermal reactor and subjected to hydrothermal treatment at 180 °C for 20 hours in an oven. After the hydrothermal process was completed, the resulting precipitate was collected, dried in an oven at 100 °C for 1 hour, and then ground using a mortar and pestle to obtain fine hydroxyapatite powder.

#### 2.2.3 Characterization of hydroxyapatite

The synthesized hydroxyapatite was characterized using various analytical techniques. Fourier-transform infrared spectroscopy (FTIR) was performed to identify functional groups present in the hydroxyapatite structure. X-ray diffraction (XRD) analysis was conducted to assess the crystallinity and phase purity of the synthesized hydroxyapatite, ensuring its compliance with ICDD standard 01-072-1243 for biomedical applications such as dental implant coatings.

TABLE 1. XRF results of ale-ale shell.

| Oxides | Concentration (%) | Oxides | Concentration (%) |
|---|---|---|---|
| $Al_2O_3$ | 0.608 | $TiO_2$ | 0.239 |
| $SiO_2$ | 1.59 | $V_2O_5$ | 0.008 |
| $P_2O_5$ | 0.899 | MnO | 0.025 |
| ClO | 0.012 | $Fe_2O_3$ | 1.93 |
| CaO | 93.444 | Others | 1.243 |

TABLE 2. Yield percentage of hydroxyapatite.

| Variation | | Initial mass (gram) | Final mass (gram) | Yield (%) |
|---|---|---|---|---|
| Ca/P concentration | pH | | | |
| 0.67 | 11 | 25.146 | 6.88 | 27.36 |
| 0.67 | 12 | 25.146 | 7.13 | 28.35 |
| 0.67 | 13 | 25.146 | 7.45 | 29.62 |
| 1.67 | 11 | 25.033 | 11.85 | 47.33 |
| 1.67 | 12 | 25.033 | 12.48 | 49.85 |
| 1.67 | 13 | 25.033 | 13.59 | 54.28 |
| 2.67 | 11 | 25.337 | 16.42 | 64.81 |
| 2.67 | 12 | 25.337 | 16.83 | 66.42 |
| 2.67 | 13 | 25.337 | 17.38 | 68.59 |

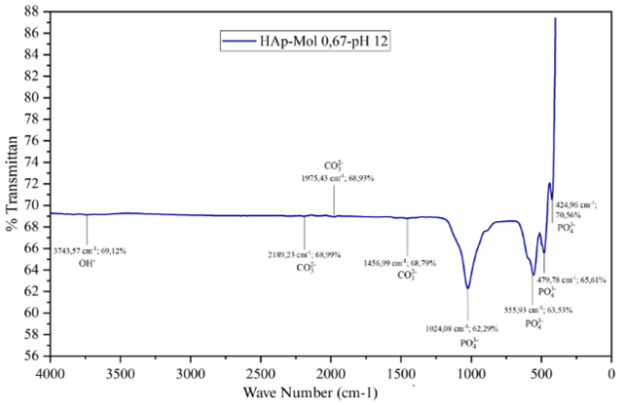


FIGURE 2. FTIR spectrum of HAp with CaO/$(NH_4)2HPO_4$ concentration ratio of 0.67 and pH 12.

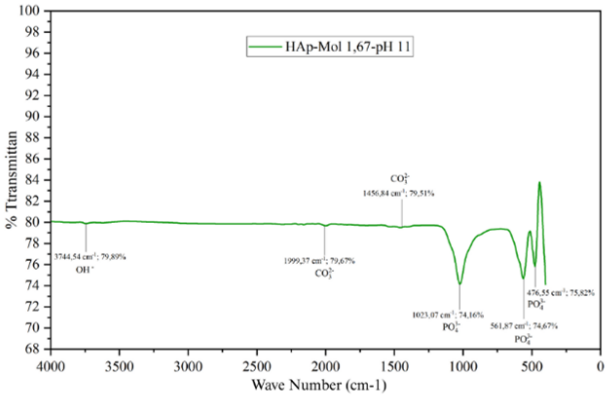


FIGURE 4. FTIR spectrum of HAp with CaO/$(NH_4)2HPO_4$ concentration ratio of 1.67 and pH 11.

## 3. RESULTS AND DISCUSSION

The research was aimed at obtaining a biomaterial of hydroxyapatite (HAp) that will be used for titanium-based dental implant coatings. Hydroxyapatite is synthesized from the shell of the ale-ale (Meretrix spp.) by hydrothermal method. The research was carried out through several stages, including sampling preparation, and HAp synthesis.

The preparation of the ale-ale shell produces CaO ashes that change color from brown to gray-white, resulting in a loss of 146 grams to 99.12 grams. LoI (Loss in Ignition) is 32.1 %. XRF analysis results can be seen in Table 1.

The largest component found in ale-ale shell powder was calcium oxide (CaO) at 93.444 %, so it can be used as a calcium precursor in hydroxyapatite synthesis.

Hydroxyapatite synthesis is carried out by hydrothermal method, which is the formation of a material using water at a temperature above the boiling point of water and high pressure to change the structure of crystals and form a nanostructure material. The hydroxyapatite, which has been successfully synthesized by hydrothermal method, was then sintered at a temperature of 800 °C for 4 hours (Byrappa K and Yoshimura 2013). The percentage of yields on the sample is

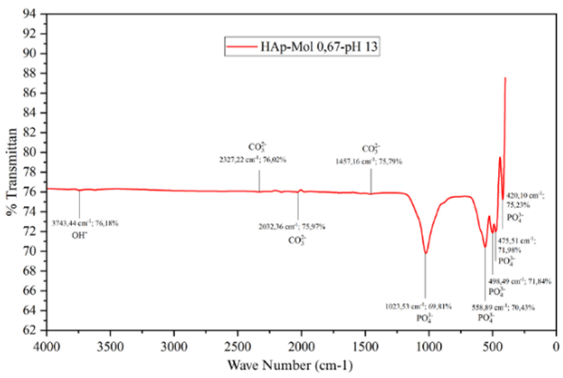


FIGURE 3. FTIR spectrum of HAp with CaO/$(NH_4)2HPO_4$ concentration ratio of 0.67 and pH 13.

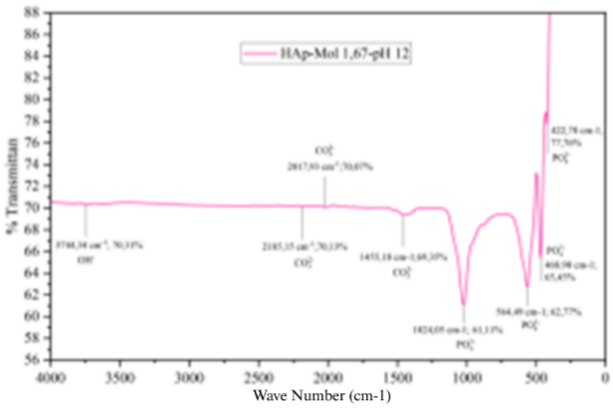


FIGURE 5. FTIR spectrum of HAp with CaO/$(NH_4)2HPO_4$ concentration ratio of 1.67 and pH 12.

performed in Table 2.

The difference in the value of % yield is influenced by the initial mass weight of the sample, which also varies with each variation in the concentration of Ca/P. The resulting value is an increasing percentage of yield with increasing concentration. This is because the lower the concentration then the solution becomes more acidic so that the hydroxyapatite compounds become more soluble and result in a low % yield at low concentrations of Ca/P. At the variation of pH also resulted in the value of % yield that increases as the pH increases. This is due to the mobility of $Ca^{2+}$ and $PO_4^{3-}$ ions which will increase with the rise of the pH thus enhancing the interaction between the molecules. The high intermolecular interaction leads to more hydroxyapatites being formed, so compared to the increased percentage of yield (Rodríguez-Lugo et al. 2018).

The synthetic hydroxyapatite was characterized using an FTIR spectroscopic photometer, with the result seen in Figure 1 - 9.

The formed groups $PO_4^{3-}$ and $OH^-$ are functional groups that are typical of HAp so indicate the HAp content in the sample. There are more sharp groups $PO_4^{3-}$, and $OH^-$ that indicate more and more content of $PO_4^{3-}$. According to Fadhilah et al. (2015), the appearance of the groups $PO_4^{3-}$ and $OH^-$ sharp indicate higher absorption intensity so indicating better HAp obtained. The appearance of the absorption of the cluster $CO_3^{2-}$ indicates the presence of the carbonate cluster of $CaCO_3$ derived from the shell of the ale-ale shell, in which the $CaCO_3$ has not been completely decomposed. Carbonate groups ($CO_3^{2-}$) can be identified in hydroxyapatite structures because of the substitution of carbonate ions with hydroxyl ions or phosphates, thus forming a carbonate-hydroxyapatite structure. The formation of such structures does not affect hydroxyapatite functions since the calcium and phosphate compounds have undergone sintering at 800 °C so that they have a stable structure (Demirkol et al. 2012). From the results of the FTIR analysis, the emergence of the three groups of these functions indicates that hydroxyapatites in the nine variations have been successfully synthesized.

Qualitative analysis of hydroxyapatite concentration ratios of 0.67; 1.67; and 2.67 at pH variations 11, 12, and 13 can be seen in Figure 11 - 12.

HAp with pH variations of 11, 12, and 13 at a concentration ratio of 0.67 with the most optimum variation based on the appearance of the sharpest $PO_4^{3-}$ group peak and the number of appearances of the $PO_4^{3-}$ namely HAp with variations in the order of pH 13, 12, and 11. HAp with variations in pH 11, 12, and 13 at a concentration ratio of 1.67 with the most optimum variation based on the appearance of cluster peaks $PO_4^{3-}$ is the sharpest and the number of occurrences of the $PO_4^{3-}$ group is HAp with the order of pH variations 13, 12, and 11. HAp with pH variations 11, 12, and 13 at a concentration ratio of 2.67 with the most optimum variation based on the appearance of the sharpest peak of the $PO_4^{3-}$ group and the number of occurrences of the $PO_4^{3-}$ group namely HAp with a pH variation sequence of 13, 12, and 11. The results of qualitative FTIR analysis on hydroxyapatite varied in concentration ratio 0.67; 1.67; and 2.67 with pH 11, 12, and 13, the most optimum variation was obtained at the HAp concentration ratio of 0.67-pH 13; HAp concentration ratio 1.67-pH 13; HAp concentration ratio 2.67-pH 13. The three variations in concentration ratio are 0.67; 1.67; and 2.67 has the most optimum results at pH 13 which is the highest pH. Based on the results of this research, it indicates that the higher the pH of the reaction, the sharper the peak of the $PO_4^{3-}$ group that is formed. At higher pH levels, calcium hydroxide ($Ca(OH)_2$) dissociates more readily, releasing a greater amount of $Ca^{2+}$ and $OH^-$ ions. The increased availability of $Ca^{2+}$ facilitates stronger interactions with $PO_4^{3-}$, accelerating the hydroxyapatite (HAp) crystallization process and enhancing its struc-

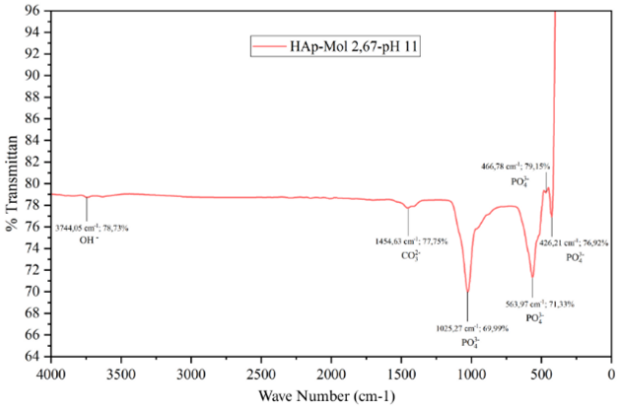


FIGURE 7. FTIR spectrum of HAp with CaO/$(NH_4)2HPO_4$ concentration ratio of 2.67 and pH 11.

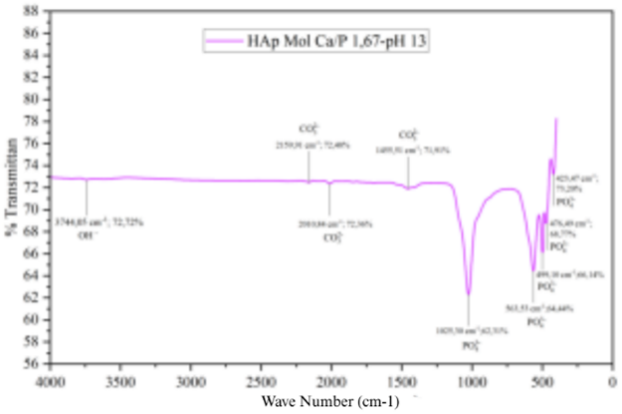


FIGURE 6. FTIR spectrum of HAp with CaO/$(NH_4)2HPO_4$ concentration ratio of 1.67 and pH 13.

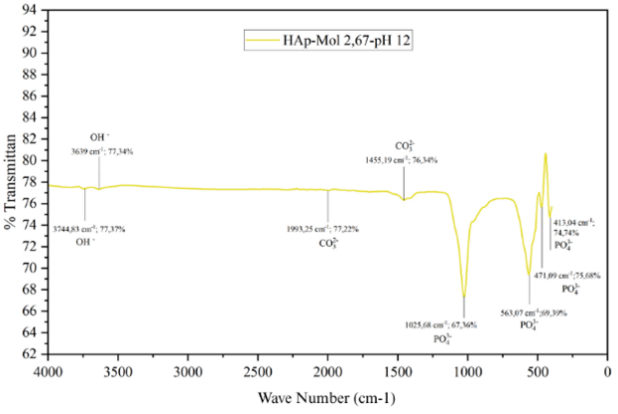


FIGURE 8. FTIR spectrum of HAp with CaO/$(NH_4)2HPO_4$ concentration ratio of 2.67 and pH 12.

DOI 10.22146/jrekpros.18186

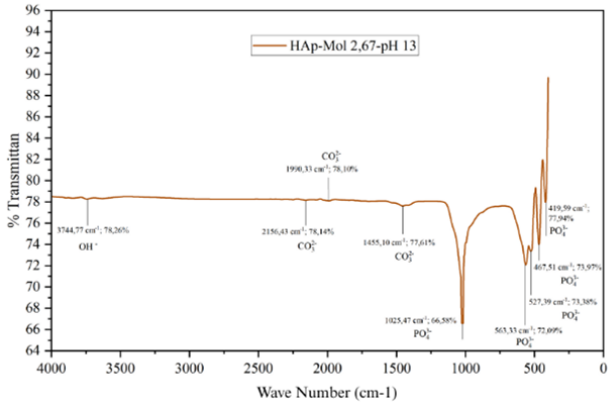


FIGURE 9. FTIR spectrum of HAp with CaO/$(NH_4)2HPO_4$ concentration ratio of 2.67 and pH 13.

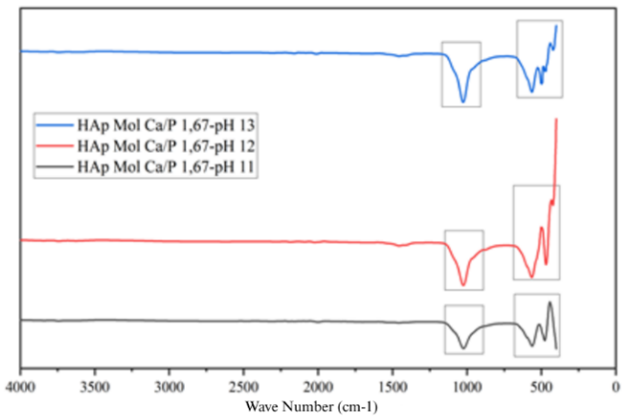


FIGURE 11. Qualitative analysis of FTIR spectrum of HAp at pH variations 11, 12, and 13 with a concentration ratio of 1.67.

tural order. This results in sharper $PO_4^{3-}$ and $OH^-$ absorption peaks in the FTIR spectrum, indicating improved crystallinity. In contrast, at lower pH levels, the release of $Ca^{2+}$ ions occurs more slowly, hindering HAp formation and leading to broader $PO_4^{3-}$ peaks. Optimal $Ca(OH)_2$ dissociation occurs at a pH range of approximately 12.5–12.8, promoting the formation of well-defined HAp crystals with higher crystallinity (Palanivelu et al. 2014).

FTIR analysis was conducted to quantify the carbonate content (% carbonate) in hydroxyapatite by measuring the absorbance of carbonate ($CO_3^{2-}$) and phosphate ($PO_4^{3-}$) functional groups. The spectra were recorded in the range of 4000–400 $cm^{-1}$, focusing on carbonate peaks at 1420–1450 $cm^{-1}$ (Type B substitution) and phosphate peaks at ~1030 $cm^{-1}$ as a reference. The carbonate content was calculated using the ratio of the absorbance or integrated area of the $CO_3^{2-}$ peak to the $PO_4^{3-}$ peak using the Equation 1.

$$\%Carbonate = \left(\frac{A_{CO_3}}{A_{PO_4}}\right) \times 100 \quad (1)$$

Where $A_{CO_3}$ represents the absorbance of the carbonate peak and $A_{PO_4}$ represents the absorbance of the phosphate peak. The results were compared with standard values of biological apatite (2–8% carbonate) to evaluate the influence of synthesis parameters on carbonate incorporation in hydroxyapatite (Rehman and Bonfield 1997). The calculation results of % $CO_3^{2-}$ can be seen in Table 3.

The results of quantitative FTIR analysis reveal that hydroxyapatite with each concentration ratio variation is 0.67; 1.67; and 2.67 at pH 13 has the smallest %$CO_3^{2-}$ value. This is because at alkaline pH there will be higher diffusion and solubility of $CO_3^{2-}$ when compared to acidic pH. The low solubility of $CO_3^{2-}$ causes carbonate ions to enter the crystal lattice, thus affecting the Ca/P ratio value of hydroxyapatite and also the crystal plane. Carbonate ions that enter the hydroxyapatite crystal lattice will replace hydroxyl ions ($OH^-$) or phosphate ($PO_4^{3-}$) and produce carbonated-HAp (CHAp) (Afshar et al. 2003). If carbonated-HAp is formed, the carbonate ion content in hydroxyapatite will increase.

Based on the calculation of % $CO_3^{2-}$ the result is that the greater the concentration ratio, the larger the value of % $CO_3^{2-}$ is obtained. This is due to the fact that this study uses an irregular Ca mass. The greater the concentration ratio, the more the CaO mass is used, so that the value of % $CO_3^{2-}$ will be greater. As CaO is used more and more, it is likely that the greater is the content of the carbonate group ($CO_3^{2-}$) in the hydroxyapatite. This is in line with the theory that the existence of carbonate groups $CO_3^{2-}$ is derived from $CaCO_3$ from the shell of ale-ale shells that have not been perfectly composed into CaO (Wathi et al. 2014). Through the results of the quantitative analysis of FTIR, it was concluded that the most

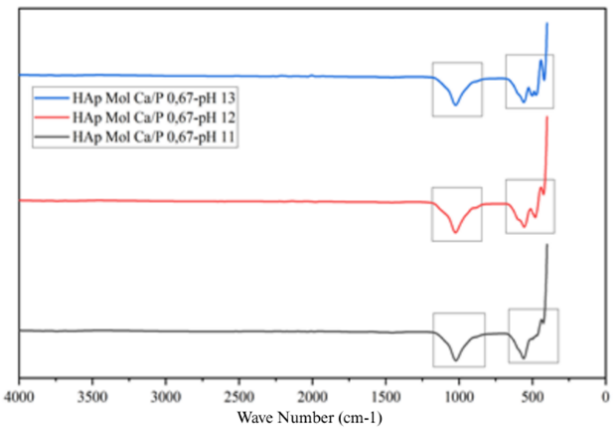


FIGURE 10. Qualitative analysis of FTIR spectrum of HAp at pH variations 11, 12, and 13 with a concentration ratio of 0.67.

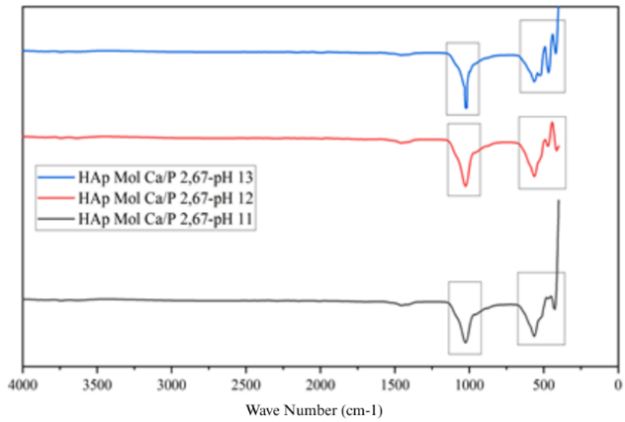


FIGURE 12. Qualitative analysis of FTIR spectrum of HAp at pH variations 11, 12, and 13 with a concentration ratio of 2.67.

TABLE 3. Percentage of $CO_3^{2-}$.

| No. | Variation | | % $CO_3^{2-}$ |
|---|---|---|---|
| | Ca/P Concentration | pH | |
| 1 | 0.67 | 11 | 0.459 |
| 2 | | 12 | 0.44 |
| 3 | | 13 | 0.402 |
| 4 | 1.67 | 11 | 1.145 |
| 5 | | 12 | 1.024 |
| 6 | | 13 | 0.831 |
| 7 | 2.67 | 11 | 1.488 |
| 8 | | 12 | 1.464 |
| 9 | | 13 | 1.323 |

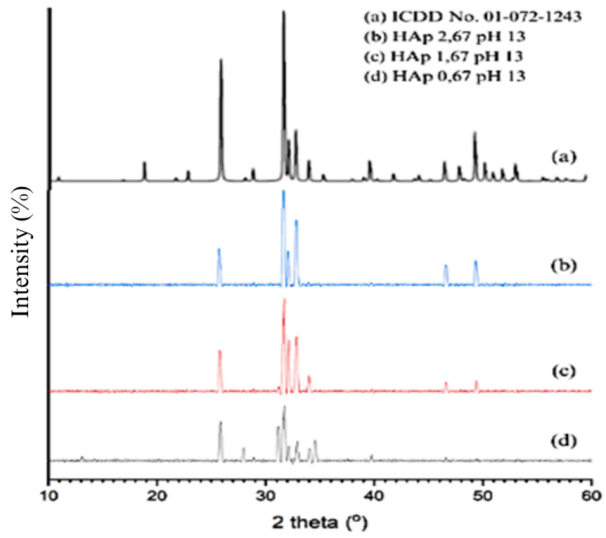


FIGURE 13. X-Ray Diffractogram of Samples with Ca/P Concentration Variations of 0.67; 1.67; and 2.67 at pH 13.

optimum hydroxyapatite synthesis was performed at pH 13. The results were in line with the qualitative analysis, with the optimum result at pH 13, then XRD analysis was done on the hydroxyapatite pH 13 with variations in the concentration ratio of 0.67; 1.67; and 2.67 to determine the most optimal hydroxyapatite based on the 2 theta angle parameters obtained through the analysis of XRD.

X-ray diffractograms on samples of Ca/P concentration variations of 0.67; 1.67; and 2.67 pH 13 in succession showed pattern compliance with ICDD HAp standard No. 01-072-1243. The XRD diffractogram pattern can be seen in Figure 13.

The three variations of hydroxyapatite have a hexagonal crystal shape. Table 4 shows the five highest peaks of XRD HAp diffractogram results compared to HAp based on ICDD 01-072-1243, but the HAp formed is not pure, as there is still another phase of tricalcium phosphate (TCP) in the synthesized HAp. At concentration variations of Ca/P 0.67 pH 13 identified TCP ($Ca_3(PO_4)$ at $2\theta$ 31.1524°and 34.5312°corresponding to the COD standard 00-009-0169. In a vessel of concentration of Ca /P 1.67 pH 13, identified TCP ($Ca_3(Po_4)$ at $1\theta$ 31.1821°. In addition to the 5 highest peaks on the XRD diffractogram, there are other angles of $2\theta$ with low intensity values so that it is detected as another phase according to the Match! program which is then considered to be a

TABLE 4. $2\theta$ Angle from XRD Analysis of Hydroxyapatite.

| HAp ICDD 01-072-1243 | | HAp pH 13 | | | | | |
|---|---|---|---|---|---|---|---|
| | | 0.67 | | 1.67 | | 2.67 | |
| $2\theta$ (°) | $I/I_0$ (%) | $2\theta$ (°) | $I/I_0$ (%) | $2\theta$ (°) | $I/I_0$ (%) | $2\theta$ (°) | $I/I_0$ (%) |
| 31.74 | 100 | 31.74 | 100 | 31.67 | 100 | 31.64 | 100 |
| 32.86 | 56.4 | 32.90 | 60.86 | 32.83 | 65.39 | 32.83 | 76.45 |
| 32.17 | 45.3 | 32.09 | 66.94 | 32.10 | 73.77 | 32.02 | 69.54 |
| 25.87 | 36.1 | 25.87 | 47.99 | 25.82 | 44.35 | 25.68 | 34.97 |
| 49.46 | 30.5 | 49.48 | 28.12 | 49.38 | 31.54 | 49.31 | 34.67 |

TABLE 5. Particle size of hydroxyapatite.

| HAp pH 13 | $2\theta$ | Crystallinity (%) | Crystal size (nm) |
|---|---|---|---|
| 0.67 | 31.74° | 87.28 | 35.25 |
| 1.67 | 31.67o° | 91.67 | 123.39 |
| 2.67 | 31.64° | 95.09 | 55.81 |

corrosion in hydroxyapatite. The forming TCP compounds are not a big problem because the most commonly used calcium phosphate is hydroxyapatite and tricalcium phosphates. HAp and TCP are bioactive and have bio-absorbable properties when implanted into the body, but HAp tends to be non-resorbable. Ideally, bio-ceramics are not only bioactive but also bio-resorbable, to give new bone tissue growth space. The combination of the bio-active properties of HAp, and the bio-resorbable characteristics of TCP with a specific composition, can better control the resorption and substitulation of bone biomaterials (Sumadi 2022).

Based on the results of the X-ray diffractogram, the crystallite size of the synthesized hydroxyapatite (HAp) can be calculated using the Scherrer equation 2

$$D = \frac{K\lambda}{\beta cos\theta} \quad (2)$$

where D represents the crystallite size, K is the Scherrer constant (typically 0.9), $\lambda$ is the X-ray wavelength (1.5406 Å for Cu K$\alpha$ radiation), $\beta$ is the full width at half maximum (FWHM) of the diffraction peak in radians, and $\theta$ is the Bragg angle (Benataya et al. 2020). The crystallite size of the synthesized hydroxyapatite, determined from the FWHM of the most intense diffraction peak, is presented in Table 5.

Crystal size less than 100 nm has better bioresorbable and bioactivity (Sumadi 2022). The magnitude of the crystal size obtained at a concentration variation of Ca/P 1.67 is due to the agglomeration or clumping of the synthetic HAp. The formation of agglomeration in the HAp result of the synthesis in this study is due to the hydrothermal processes carried out not using the condensation system so that the distribution of particles is less homogeneous.

The optimum HAp in this study was obtained at a concentration ratio of Ca/P 2.67 which has a crystallinity of 95.09 %, where this is the largest crystallinity value of the other two concentration ratios. In addition, the hydroxyapatite of the concentration rate of Ca/P 2.67 has a particle size of 55.81 nm, which is >100 nm, so it has better bioresorbable and bioactivity. In HAp, the concentrations ratio Ca/P 0.67 has smaller particle sizes than the HAp ratio ca/P 2.67, which is 35.25 nm, but HAp has a small crystalline value of 87.28 %.

## 4. CONCLUSION

Based on the results of the research, it can be concluded that hydroxyapatite-based shell of ale-ale (Meretrix spp.) containing calcium (Ca) of 93.444 % has been successfully synthesized using hydrothermal methods. The XRF data on the calcined ale-ale shell indicates the presence of CaO that can be used as a precursor for the substance of Hap synthesis. Based on the FTIR analysis of each sample of synthetic HAp, there are $PO_4^{3-}$, $OH^-$, and $CO_3^{2-}$ groups indicating the hydroxyapatite content of the sample. The formation of major HAp peaks on XRD data that corresponds to ICDD 01-072-1243 standard data has reinforced the truth related to the formation of HAp. Hydroxyapatite synthesis with ale-ale shell waste raw materials by hydrothermal method gives the best results at a concentration ratio of Ca/P 2.67-pH 13 with a crystallinity of 95.09% and a hexagonal crystal size of 55.81 nm.

## 5. ACKNOWLEDGMENT

We would like to thank the Ministry of Education, Culture, Research and Technology of the Republic of Indonesia for its support and funding. Besides, we would also like to thank Tanjungpura University for providing facilities and technical guidance so that this research can be completed well.

## REFERENCES

Affandi A, Amri A, Zultiniar Z. 2015. Sintesis hidroksiapatit dari cangkang kerang darah (Anadara granosa) dengan proses hidrotermal variasi rasio mol Ca/P dan suhu sintesis. Jurnal Online Mahasiswa Fakultas Teknik Universitas Riau. 2(1):1–8. https://jom.unri.ac.id/.

Afshar A, Ghorbani M, Ehsani N, Saeri M, Sorrell C. 2003. Some important factors in the wet precipitation process of hydroxyapatite. Materials & Design. 24(3):197–202. doi:10.1016/S0261-3069(03)00003-7.

Benataya K, Lakrat M, Elansari L, Mejdoubi E. 2020. Synthesis of B-type carbonated hydroxyapatite by a new dissolution-precipitation method. Materials Today: Proceedings. 31:S83–S88. doi:10.1016/j.matpr.2020.06.100.

Byrappa K, Yoshimura M. 2013. Handbook of hydrothermal technology. Elsevier. doi:10.1016/C2009-0-20354-0.

Demirkol N, Oktar FN, Kayali ES. 2012. Mechanical and microstructural properties of sheep hydroxyapatite (SHA)-niobium oxide composites. Acta Physica Polonica A. 121(1):274–276. doi:10.12693/APhysPolA.121.274.

Fadhilah R, Kurniawan RA, Icha MM. 2015. Sintesis hidroksiapatit dari cangkang kerang ale-ale (Meretrix spp) sebagai material graft tulang. Jurnal Buletin Al-Ribaath. 12(1). doi:10.29406/br.v12i1.79.

Palanivelu R, Mary Saral A, Ruban Kumar A. 2014. Nanocrystalline hydroxyapatite prepared under various pH conditions. Spectrochimica Acta Part A: Molecular and Biomolecular Spectroscopy. 131:37–41. doi:10.1016/j.saa.2014.04.014.

Rehman I, Bonfield W. 1997. Characterization of hydroxyapatite and carbonated apatite by photo acoustic FTIR spectroscopy. Journal of Materials Science: Materials in Medicine. 8(1):1–4. doi:10.1023/A:1018570213546.

Rodríguez-Lugo V, Karthik TVK, Mendoza-Anaya D, Rubio-Rosas E, Villaseñor Cerón LS, Reyes-Valderrama MI, Salinas-Rodríguez E. 2018. Wet chemical synthesis of nanocrystalline hydroxyapatite flakes: effect of pH and sintering temperature on structural and morphological properties. Royal Society Open Science. 5(8):180962. doi:10.1098/rsos.180962.

Sianipar JS, Azis Y, ' Z. 2016. Sintesis hidroksiapatit melalui precipitated calcium carbonate (PCC) kulit kerang darah dengan metode hidrotermal. Jurnal Online Mahasiswa Fakultas Teknik Universitas Riau. 3(2):1–7. https://jom.unri.ac.id/.

Souza JC, Sordi MB, Kanazawa M, Ravindran S, Henriques B, Silva FS, Aparicio C, Cooper LF. 2019. Nano-scale modification of titanium implant surfaces to enhance osseointegration. Acta Biomaterialia. 94:112–131. doi:10.1016/j.actbio.2019.05.045.

Sumadi R. 2022. Sintesis dan karakterisasi membran komposit dari hidroksiapatit kerang dara-kitosan sebagai aplikasi biokomposit. [Bachelor thesis]: Universitas Jambi.

Wathi AFD, Wardhani S, Khunur MM. 2014. Pengaruh perbandingan massa Ca:P terhadap sintesis hidroksiapatit tulang sapi dengan metode kering. Jurnal Ilmu Kimia Universitas Brawijaya. 1(2).